Tunnelling and Underground Space Technology 74 (2018) 1–9

Contents lists available at ScienceDirect

Tunnelling and Underground Space Technology

journal homepage: www.elsevier.com/locate/tust

Seismic performance upgrading for underground structures by introducing sliding isolation bearings

Ma Chao[a,b], Lu Dechun[a,*], Du Xiuli[a,*]

[a] Institute of Geotechnical and Underground Engineering, Beijing University of Technology, Beijing, China
[b] School of Civil and Transportation Engineering, Beijing University of Civil Engineering and Architecture, Beijing, China

ARTICLE INFO

Keywords:
Sliding isolation bearings
Underground structures
Collapse mechanism
Deformation capacity
Seismic performance

ABSTRACT

Isolation bearings have been a widely applied seismic strengthening technique in above ground structures. Whereas, the sliding isolation bearings were seldom used in underground structures. This study aims to explore the feasibility of sliding isolation bearings reducing the seismic response of underground structures. The collapse mechanism of underground structures was firstly analyzed by taking the Daikai Station as an example. Numerical results demonstrated that the collapse of the structure was due to the poor ductility of the intermediate columns. Therefore, the sliding isolation bearing could be installed between the columns and the beam to reduce the lateral deformations of columns. In order to determine an appropriate coefficient for sliding bearings, static analyses for the capacity of columns were conducted. Moreover, the performances of a beam-bearing-column system were also investigated. Finally, seismic responses of the underground structure retrofitted with bearings were studied. Numerical results presented that the responses of both columns and the whole structure were reduced remarkably. Moreover, the frictional coefficient of bearing influencing the seismic responses of underground structures was discussed. And some interesting conclusions were also obtained for the seismic design of underground structures.

1. Introduction

The construction of underground structures including subway stations, underground malls, tunnels, and underground parking stations has gained a rapid development in China during recent years. Taking the subway stations as the example, more than 2000 stations along the total of 3000 km long tunnels have been constructed till 2015 (Chen et al., 2016), and up to 373 stations were constructed in 2016. However, almost all the cities with underground structures in China are in the strong earthquake prone area. Seismic investigations showed that underground structures were at greater risk during an earthquake (Sharma and Judd, 1991; Yashida and Nakamura, 1996; Wang et al., 2000; Wang et al., 2009; Shen et al., 2014; Lee et al., 2016). Therefore, it is of urgent need to focus on the seismic safety and seismic design of underground structures.

Seismic isolation technology is an approach that adding an isolation system between structures and the foundation, and is an effective way to reduce earthquake energy transferring from ground to structure (Providakis, 2009; Li and Li, 2011). This technology as an approach to earthquake protection has been used more than 100 years (Buckle and Mayes, 1990) in above ground structures. Seismic isolation technology has been introduced to underground structures aiming to reduce the damage of underground structures during an earthquake (Xin et al., 2014; Li, 2012) in recent years. The isolation layer was applied as the buffering to mitigate the constraint of the surrounding ground, and then the earthquake-induced structural deformation and forces of underground structures were reduced (Xin et al., 2014). The isolation layer was always used for the seismic design of tunnels (Suzuki, 2000; Kim and Konagai, 2001; Konagai and Kim, 2001; Hasheminejad and Miri, 2008; Kiryu et al., 2012; Chen and Shen, 2014; Wang et al., 2017). Moreover, seismic investigations and damage features of tunnels from the Wenchuan earthquake also illustrated that isolation layers could be applied to improve the seismic performance of tunnels (Li, 2012). Studies proved that seismic isolation technology was an effective way of reducing damages to tunnels. Alternatively, seismic reduction technology is another approach to protecting structures surviving during an earthquake, and has also been applied in the underground structures. For example, flexible joints were utilized between the segments of tunnels to mitigate the earthquake-induced stress concentration (Ding et al., 2006; Yu et al., 2013; Do et al., 2015; Kawamata et al., 2016; Yu et al., 2017).

Analyses of seismic responses of underground structures presented

* Corresponding authors.
E-mail addresses: machaowater@126.com (C. Ma), dechun@bjut.edu.cn (D. Lu), duxiuli@bjut.edu.cn (X. Du).

https://doi.org/10.1016/j.tust.2018.01.007
Received 26 April 2017; Received in revised form 2 January 2018; Accepted 5 January 2018

that intermediate columns were the key structural components (Hashash et al., 2001; Huo et al., 2005; Nam et al., 2016; Ma et al., 2017b). Failure of intermediate columns could result in the collapse of underground structures. Thus, the isolation bearings were also used as the damper installed between the columns and beams to weaken the seismic responses of underground structures. In consideration of the survivability of the Daikai Station from the great lateral deformation, a 3D shock isolator bearing composed of dish spring and lead rubber beading was introduced to reduce the lateral deformation of column (Huan et al., 2011). Numerical results presented that the 3D shock isolator could reduce the lateral deformation and damage of columns. A flexible rubber joint was inserted on upper and/or lower ends of columns to updating the seismic performance of the Daikai station (Mikami et al., 2001). It demonstrated that the induced shear force and moment of columns were also weakened. Similarly, a shear panel damper bearing was installed between the top beam and columns to upgrade the seismic performance of underground structures (Chen et al., 2014). It demonstrated that the maximum shear forces of columns in both single- and double-story structures declined effectively although the lateral deformation of columns increased. However, during the studies of Mikami et al. (2001), Huan et al. (2011) and Chen et al. (2014), the lateral deformation of columns changed slightly during earthquake. Because the functionality of columns is to bear vertical loadings, more effective measures which could keep the columns standing upright, should be ultimate to reduce the deformation of columns and to promote the seismic responses of underground structures.

Sliding isolation bearing is a typical type of passive seismic isolation devices. Sliding isolation bearings are capable of changing stiffness property during the horizontal flexibility. The bearings provide protection against earthquakes by reducing the peak and residual displacement of buildings (Nagarajaiah et al., 1993; Mualla and Belev, 2002; Fenz and Constantinou, 2006; Castaldo et al., 2015). When the bearings are installed between beams and columns of underground structures, the deformation of columns will be transferred to the slide of the bearings. Therefore, in this study, sliding isolation bearings were utilized to underground structures for updating the seismic response. The collapse mechanism of underground structures was firstly analyzed by taking the Daikai Station as an example. Then the recommended optimum range of the frictional coefficient of sliding isolation bearings was determined by carrying out the ductility of columns under different normalized force. To assess the seismic performance of underground structures retrofitted with sliding bearings, nonlinear dynamic analyses were conducted, and a discussion about the seismic improvement of underground structures was also presented, which may be a useful references for future design.

2. Failure mechanism of underground structures

2.1. Target structure and numerical model

During the Great Hanshin earthquake, on 17 January 1995, more than 30 intermediate columns (in total 35 columns) of the Daikai Station completely collapsed over a total length of about 110 m. The largest subsidence of the ground reached 2.5 m. This station is the only collapse underground structure during an earthquake. The collapse of the Daikai Station attracted great interest of researchers and engineers, and this station was always represented as an example to study the failure mechanism of underground structures (Iida et al., 1996; Yashida and Nakamura, 1996; Hashash et al., 2001; Huo et al., 2005).

In this section, the completely collapse section of the Daikai Station is selected as the research target to study the collapse mechanism of underground structures. Then a 3D FEM model with dimensions of 80 m long, 20 m width and 30 m high was built for the nonlinear numerical analysis, as shown in Fig. 1. According to Liao's (2013) study, the maximal height of element h_{max} of the shear motion propagating in the soil should be determined by

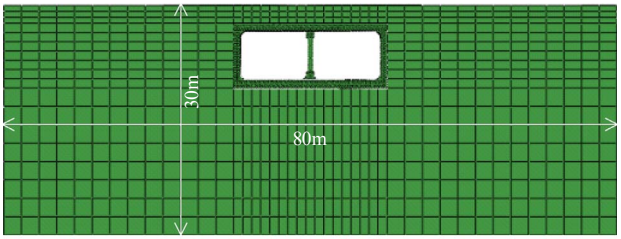

(a) Transverse section of the FEM model

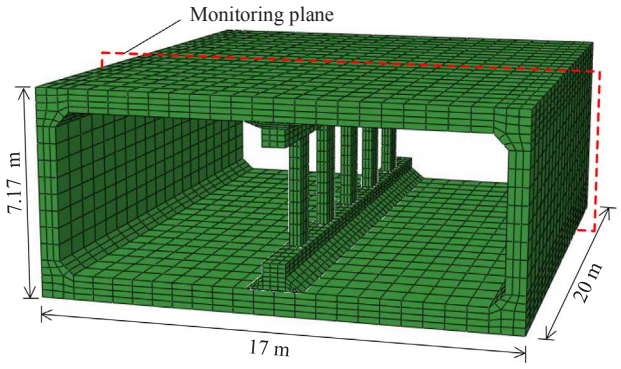

(b) 3D FEM model of structure

Fig. 1. FEM numerical model.

$$h_{max} = (1/75 \sim 1/160)V_s/f_{max} \quad (1)$$

where, V_s is the shear and compression motion velocity, which can be deduced by Eq. (2).

$$G = \rho V_s^2 \quad (2)$$

where, ρ is the density of the soil. f_{max} is the maximal vibration frequency of the input motion, which is 0.82 Hz. The viscoelastic artificial boundary conditions were utilized to deal with the lateral and bottom boundaries in order to decrease the influence caused by infinite field. On the basis of the viscoelastic boundary condition, the wave field decomposition method was used to implement the seismic input. During the simulation, the horizontal and vertical components of ground motions shown in Fig. 2 were applied, which were measured at the Kobe meteorological observatory closing to the Daikai Station. Noting that, both the horizontal and vertical components of ground motion are at a very high level. However, the amplitudes of both ground motions decrease to no larger than 0.1 g after 20.0 s. Therefore, a period of the previous 23.0 s simulation was carried out.

The concrete in the structure was modeled as the plastic damage model, with density 2500 kg/m^3, Poisson's ratio 0.2, Young's modulus 30 GPa, initial compression yield stress 18.8 MPa, limited compression yield stress 26.8 MPa, and initial tensile yield stress 2.4 MPa. An elastoplastic constitutive model developed for soil (Lu et al., 2017; Ma et al., 2017a,b) was used to describe the 3D strength, strain softening and the behaviour under monotonic and cyclic loading, with the density ρ = 1900 kg/m^3, frictional angle φ = 35°, Poisson's ratio υ = 0.3, initial pore ratio e_0 = 0.6, the isotropic compression index λ = 0.12 and the swelling index κ = 0.008. The initial consolidation pressure p_0 of ground increases from 1.5 MPa at the surface to 3.0 MPa at the bottom. For the soil, the Yong modulus E is expressed as:

$$E = 3(1-2\upsilon)\frac{1+e_0}{\kappa}p_0 \quad (3)$$

And $G = E/2(1+\upsilon)$. Then according to Eqs. (1)–(3), the range of the maximal element height h_{max} of the soil can be deduced as 2 m–4 m for the ground surface and 4 m–8 m for the bottom. Here, the lower

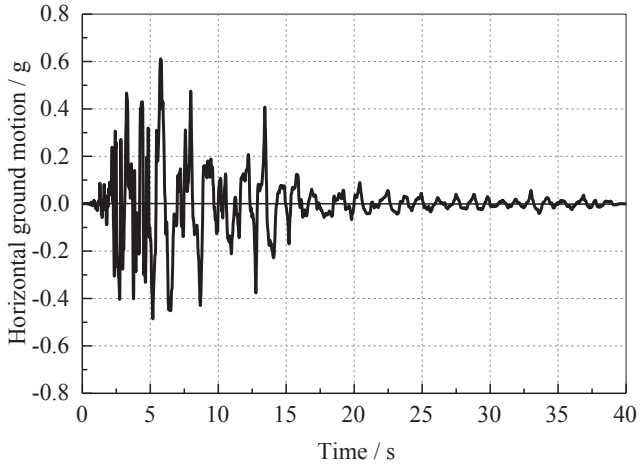

(a) Horizontal ground motion

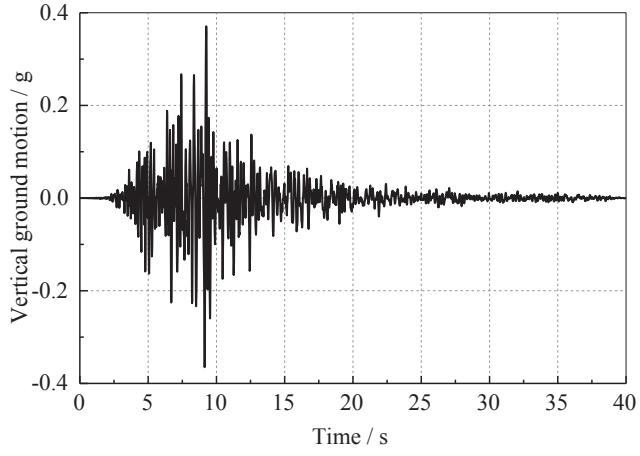

(b) Vertical ground motion

Fig. 2. Ground acceleration time history.

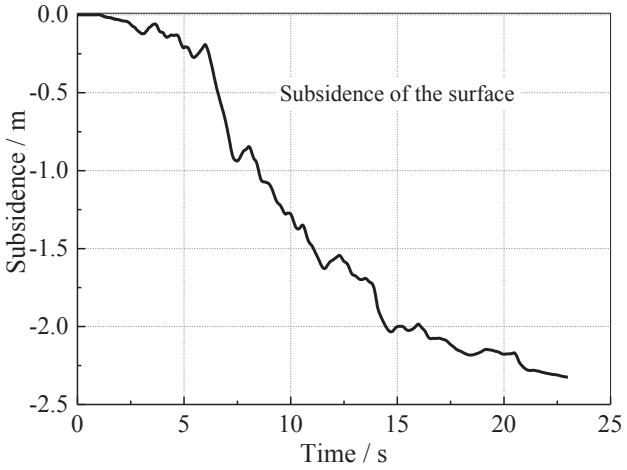

(a) Ground subsidence

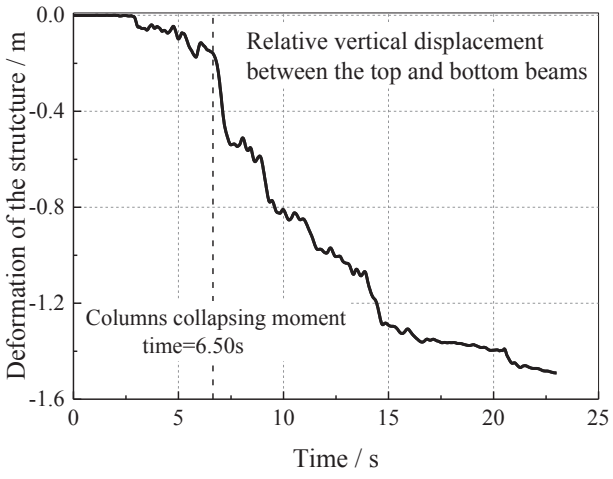

(b) Deformation of the structure

Fig. 3. Deformation time history of the structure and soil.

value of each range were used to mash the FEM model. Then the element height of the soil ranges from 2 m to 4 m. The steel in the structure was modeled as the ideal elastoplastic model, with density 7800 kg/m^3, Poisson's ratio 0.1, Young's modulus 200 GPa, yield stress 240 MPa. The Coulomb's friction law was used to simulate the behaviour of the interface between structure and ground. Referring the study of Huo et al. (2005) and Ma et al. (2017b), the friction coefficient between soil and structure was set as 0.4, and no cohesion between structure and ground was included.

2.2. Failure mechanism analysis

Fig. 3(a) presents the time histories of ground subsidence and relative vertical displacement between the ceiling and floor of the Daikai Station. With the duration of seismic loading, both the ground subsidence and the deformation of the structure increased. At the end of the seismic loading, the ground subsidence reached its maximum value (2.324 m), which approximates to the seismic investigations (Yashida and Nakamura, 1996). The final relative vertical displacement between the ceiling and floor is about 1.491 m, which indicates that the structure has been destroyed. The final deformation of structure, shown in Fig. 4(a), presents that the whole structure exhibits a vertical failure mode. In particular, the intermediate columns were bent, ceiling slab was broken, the top beam and the ceiling slab fell down. The ceiling slab and walls collapsed to an "M" failure mode. Comparisons between the obtained failure model and the seismic investigation shown in

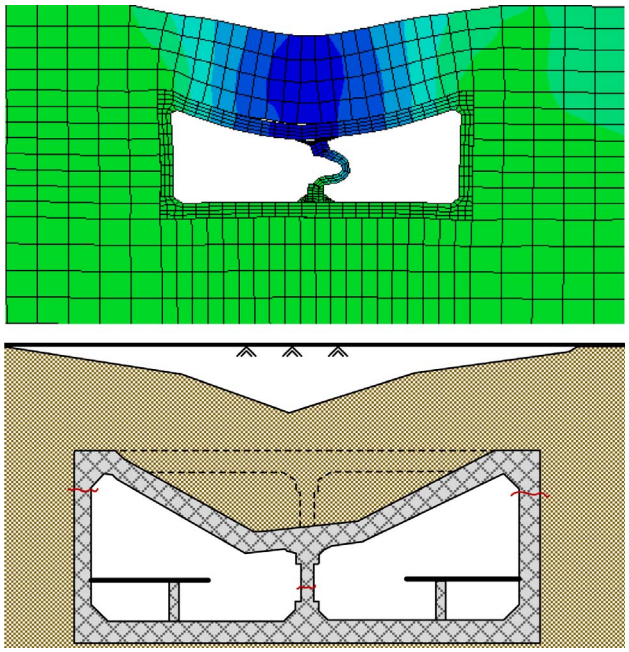

Fig. 4. Comparison between numerical result and investigation.

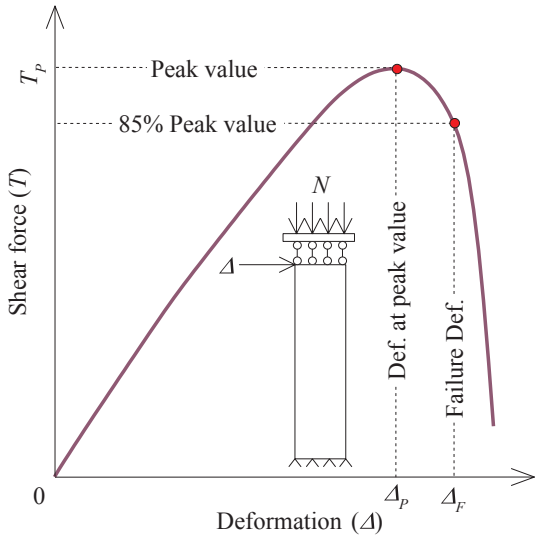

Fig. 5. Loading scheme and failure standard of the components.

Fig. 4(b) indicate that, the numerical results are in good agreement with the investigation. Therefore, it can be concluded that the failure procedure of the Daikai Station was reappeared.

The relative vertical displacement between the ceiling and floor is used as the indicator to judge the collapse of the structure. Noting that, there is an inflection point on the curve of the relative vertical displacement between the ceiling and floor at 6.50 s. Since then, the relative displacement increases monotonously and rapidly, shown in Fig. 3(b). The relative displacement has a 0.39 m increase during the following second. Therefore, the collapsing of the structure begins at 6.50 s.

A number of researches (Iida et al., 1996; An et al., 1997; Huo et al., 2005) indicated that the collapse of the Daikai Station began from the failure of the intermediate columns. To clearly explain the failure mechanism of the structure, several static analyses were carried out by using the pushover method. The corresponding loading scheme is shown in Fig. 5. During the analyses, the bottom of the components, including the column and lateral wall, was fixed. After a constant axial force N acted on the top of components, horizontal displacement at the top of the components was then incrementally increased. Shear force-deformation (T−Δ) curve, shown in Fig. 5, can be obtained in each test. Herein, shear force T is the reaction force monitored at the bottom of components. The failure of components is defined as when T fell to 85% of its peak value, and the corresponding deformation is Δ_F. After simulating the failure process of the column and lateral wall at various axial force, shear force-deformation curves were obtained and plotted in Fig. 6. The numbers on the curves in Fig. 6 are the corresponding normalized forces. Here, normalized force N_c is defined as:

$$N_c = \frac{N}{\sigma_d A} \tag{4}$$

where, σ_d is the concrete strength for design and A is the sectional area of components. The obtained loading capacity which is ○ presented in Fig. 6 were used to give the envelopes of the column and wall presented in Fig. 7. Fig. 7 illustrates that the rising of N_c in column and wall weakens their lateral deformation capacity.

Fig. 7 also presents the seismic responses of the columns and the lateral walls. Both the deformation and the normalized force of the column and lateral walls were obtained from the monitoring plane shown in Fig. 1(b). The seismic responses of the column and lateral walls in the following were also obtained from the monitoring plane shown in Fig. 1(b). The initial N_c of the columns and walls are 0.48 and 0.08, respectively. During the earthquake, the maximum N_c value of the column reaches to 0.72; whereas, the maximum N_c value of the lateral

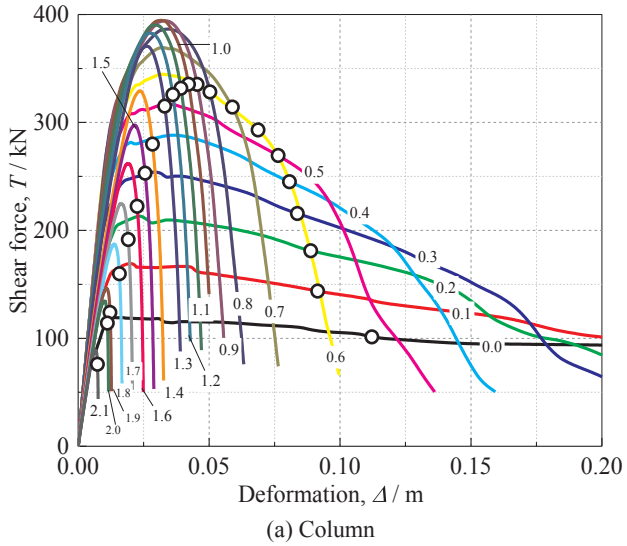

Fig. 6. Shear force-deformation curves.

walls is not greater than 0.1. Therefore, the column works at the high N_c value state with poor ductility, while the walls work at the low N_c value state with excellent ductility. Consequently, the lateral deformation capacity of the column becomes rather smaller and is far lower than that of the walls. At the failure moment (6.50 s), the lateral deformation of the columns is 0.062 m. However, for the lateral walls, the lateral deformations are not larger than 0.053 m. The deformations of the column and walls are almost the same size, however, the deformation of the column is far beyond its failure envelope, whereas, the deformations of walls are locating within their capacity. Thus, the collapse of the structure is from the failure of the column. In conclusion, the collapse of the Daikai Station originates from the poor ductility of the column at the high normalized force state.

Fig. 8 shows the time histories of total loads bearing by all the columns. From the beginning of earthquake to 6.50 s, the vertical loads bearing by the columns are around 35%–45% of the total vertical loads acting on the structure. However, the horizontal loads bearing by all the columns are no more than 8% of total ones. In this sense, the main functionality of columns in underground structures is to support the vertical loads. Moreover, Fig. 7 also presents that the vertical loads acting on the column are far below its maximum vertical loading capacity. Therefore, the way keeping the columns upright can be applied to rescue the underground structure during an earthquake.

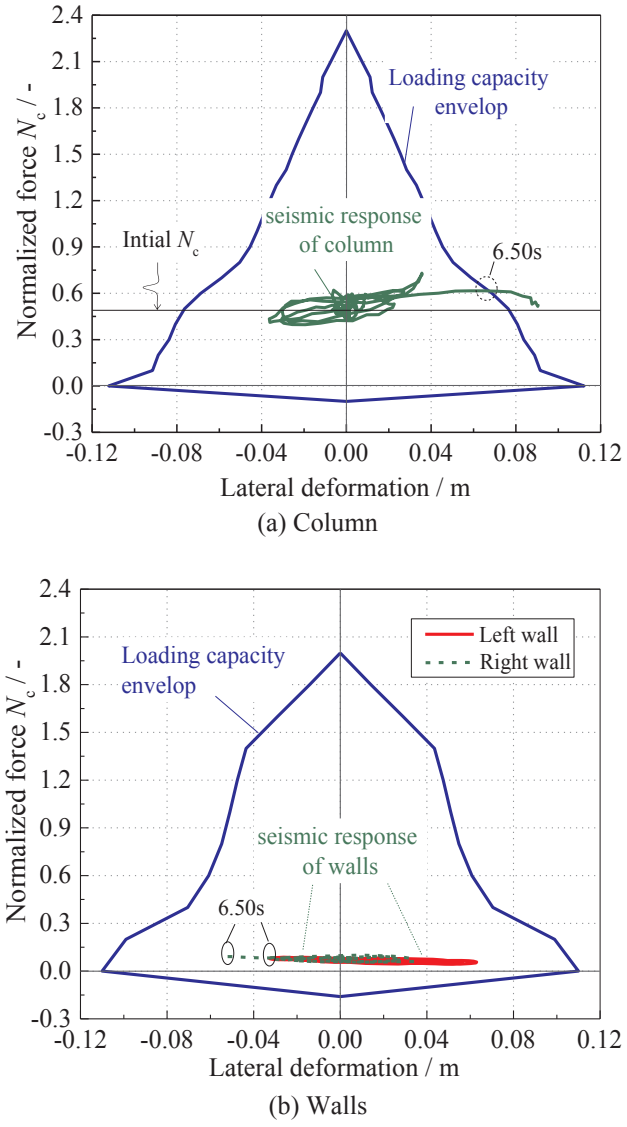

Fig. 7. Seismic response of structure and capacity envelops of components.

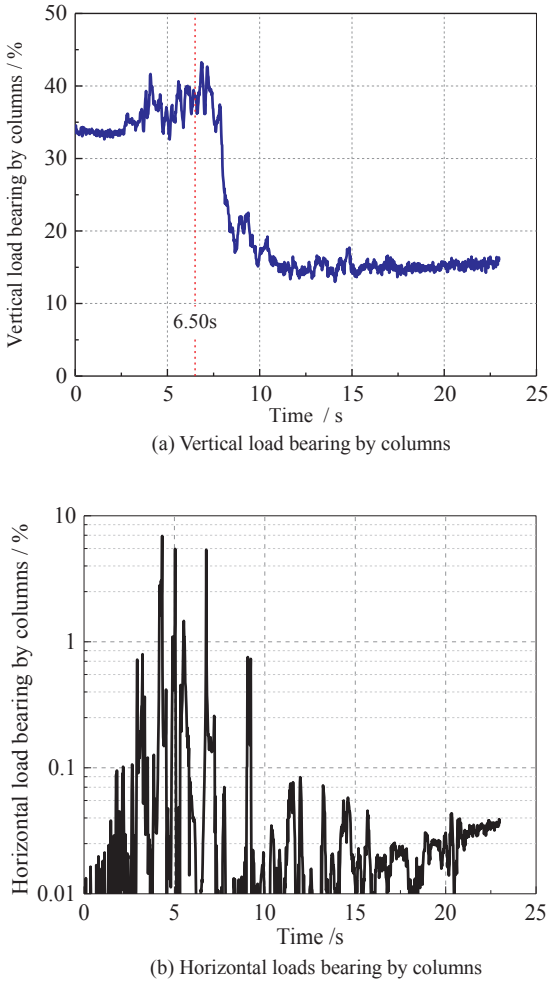

Fig. 8. Time histories of total loads carrying by the columns.

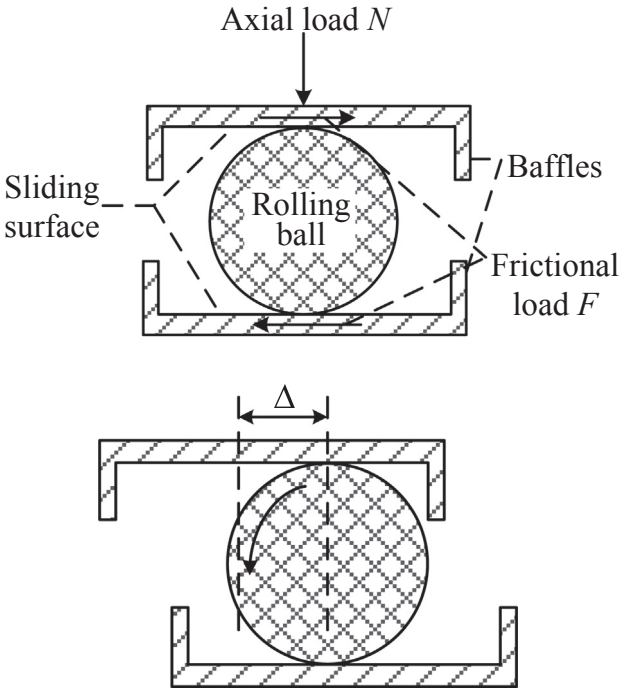

Fig. 9. Schematic diagram of the Pure-Friction-System bearing.

3. Sliding isolation bearings application in underground structures

3.1. Sliding isolation bearings

Pure-Friction-System without any restoring force is the simplest sliding system device. The typical Pure-Friction-System bearing was used in this study, which schematic diagram is presented in Fig. 9. In Fig. 9, the F is the friction force before sliding occurring when N is an instant, the value of F is given by

$$F = f(N) \tag{5}$$

where, N is the normal force acting across the sliding interface. f is the function of instantaneous values of sliding velocity, the normal force on the bearing and temperature at the sliding surface, etc. Moreover, f is also influenced by the contact type and material of isolation bearings. When the friction force reaches to F, the rolling ball moves along the sliding surface, relative displacement will be accrued between the sliding surfaces. Consequently, the ductility demand for the components will be satisfied. Every time the sense of sliding reverts, the direction of F also changes. The frictional force at the interface is always described using Coulomb type friction. Due to their inherent flexibility in the horizontal direction, the Pure-Friction-System bearings have the

capacity to undergo large displacements when subjected to strong ground motions (Berger, 2002; Ismail et al. 2010).

3.2. Determination of frictional coefficient

Different from isolating the underground structures from the surrounding ground, Pure-Friction-System bearings applied in underground structures is to separate structural components. Considering the seismic failure mechanism of underground structures, Pure-Friction-System bearing will be installed between the capital of column and the top beam. The functionality of bearings in underground structures is to reduce the lateral deformation of columns not to the dissipate seismic energy. Therefore, it is important to obtain the maximum horizontal deformation of columns for giving a recommended optimum range of the friction coefficient.

Fig. 7(a) shows that columns work in the state of $0.4 < N_c < 0.8$ during the earthquake. Therefore, the relations between lateral deformation and lateral shear force of column under normalized forces of 0.3, 0.4, 0.5, 0.6, 0.7 and 0.8 were used to determine the sliding coefficient. The corresponding normal forces, the obtained maximum lateral shear loads and maximum lateral deformation are all demonstrated in Table 1. The ratios between maximum shear forces and corresponding normal forces were also calculated and presented in Table 1. Consequently, the maximum horizontal deformation of the columns must be smaller than 0.050 m, accordingly, the sliding coefficient should be smaller than 0.076 when using a sliding isolation bearing to enhancing the seismic performance of the Daikai Station.

Pure-Friction-System bearings were installed between the capital of columns and the top beam presented in Fig. 10. Then, a serious of static numerical tests were conducted with the normalized force 0.6 (axial load 3240 kN) to study the effect of the beam-isolation-column system. During the numerical simulations, the coefficient of friction is kept as a constant 0.02, and the beam-bearing-column system was subjected to constant axial load as the beam goes under cyclic lateral loads. The simulation results are exhibited in Fig. 11. When the lateral force reaches 64.8 kN, the bearing begins slid. At this time, the deformation of the column is only 0.040 m, which is rather smaller than the deformation capacity of the column shown in Fig. 5 and Table 1. Then both the deformation of the column and shear force no longer increased. Therefore, the sliding bearings could be used to reduce the deformation of the column and enhance the performance of the Daikai Station.

4. Seismic resistance analysis and discussion

The Pure-Friction-System bearings with $\mu = 0.02$ discussed above were installed between all the columns and the top beam to simulate the seismic response of the Daikai Station. During the simulation, the friction coefficient is independent of velocity, axial load, etc. In addition, the seismic loads, constitutive model for materials, interactions as well as boundary conditions are the same as that in Section 2. The obtained numerical results are used to analysis the seismic resistance of underground structures.

Fig. 12 presents the comparison of the vertical relative deformation of the beams between the structures with and without sliding bearings. The maximum relative deformation of the structure retrofitted with bearings is no larger than 0.026 m, which is relatively smaller than 1.491 m of the structure without retrofitted. Note that the seismic responses of the column and lateral walls were also obtained from the monitoring plane shown in Fig. 1(b). Numerical results indicate that sliding bearings are an effective way to enhancing the seismic performance of underground structures. In order to comprehend detailedly about seismic efficiency of frictional bearings in the underground structure, the seismic responses of the column and whole structure are analyzed following.

Table 1
Sliding coefficient under different normalized forces.

Normalized force/–	0.3	0.4	0.5	0.6	0.7	0.8
Normal force/kN	1620	2160	2700	3240	3780	4320
Maximum lateral deformation/m	0.084	0.081	0.076	0.069	0.059	0.050
Maximum shear force/kN	215	245	269	293	314	328
Sliding coefficient/–	0.133	0.113	0.100	0.090	0.083	0.076

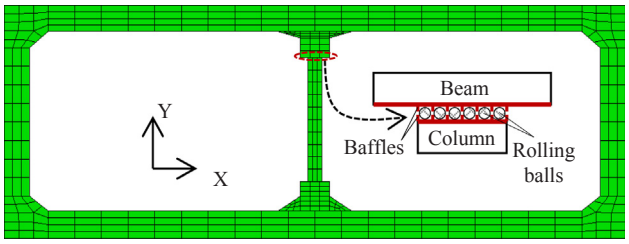

Fig. 10. FEM model of the beam-bearing-column system.

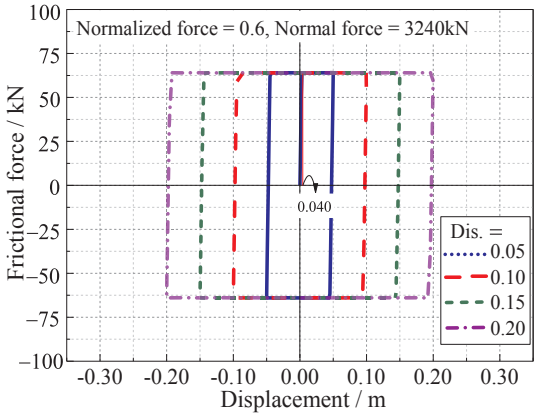

Fig. 11. Force-displacement of the beam-bearing-column system with four loading hoops.

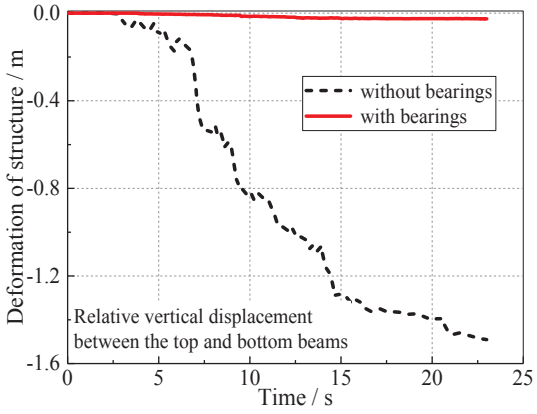

Fig. 12. Vertical relative displacement between the top and bottom beams.

4.1. Seismic response of columns

Numerical simulation presents that the lateral deformation of the column was reduced by adding sliding bearings to the underground structure. Fig. 13(a) shows the comparisons of the lateral deformation time histories of the column between structures with and without retrofitted with bearings. At 6.5 s, which is the collapsing moment of the structure without retrofitted, the lateral deformation of the column without retrofitted is 0.090 m. However, at this moment, the lateral deformation of the column with bearings is only 0.036 m. The deformation of the column reduced by the bearing is obvious. Moreover,

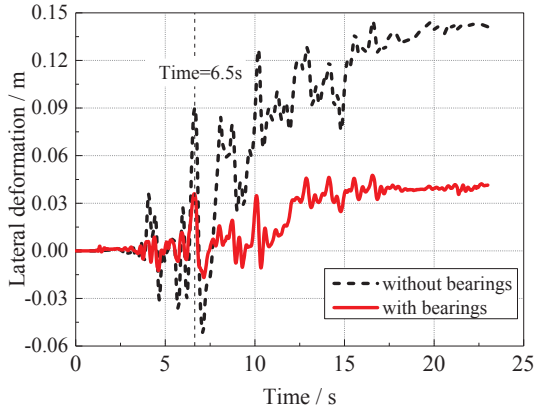

(a) Lateral deformation time histories of the column

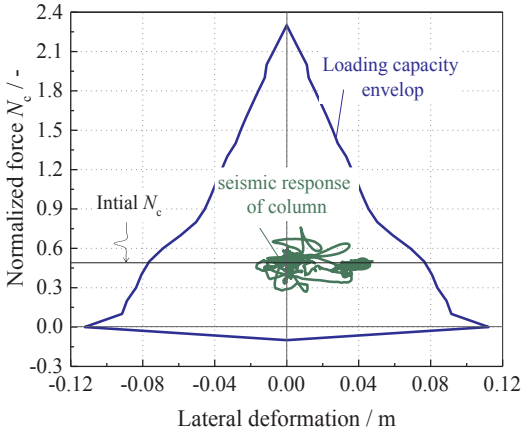

(b) Seismic response and loading capacity of the column

Fig. 13. Seismic response of the column.

during the earthquake, the maximum lateral deformation of the column with bearings is 0.048 m. 0.048 m is slight larger than 0.040 m which is from the static numerical tests. This is because, the deformation of the column accumulates during the earthquake. Obviously, the columns will exist residual deformation after seismic loads, which is about 0.041 m. Although the normalized force of column changes comparing with that shown in Fig. 7(a), the seismic response of column is located within the loading capacity envelope. Therefore, the column does not fail during the earthquake. Further, it can be concluded that the underground structure does not collapse during the earthquake according to the failure mechanism of the underground structure.

Fig. 14 presents the sliding displacement of the isolation bearing. The maximum sliding displacement is 0.054 m around 5.5 s of the

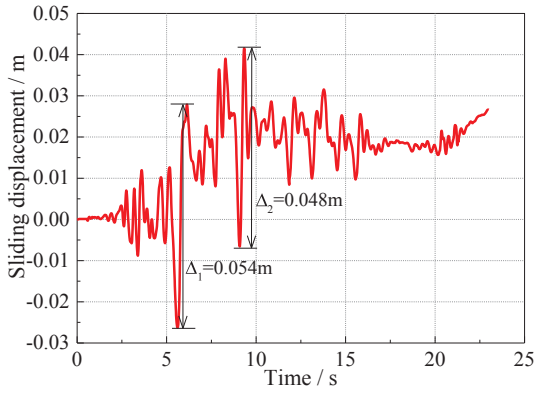

Fig. 14. Sliding displacement of the isolation bearing.

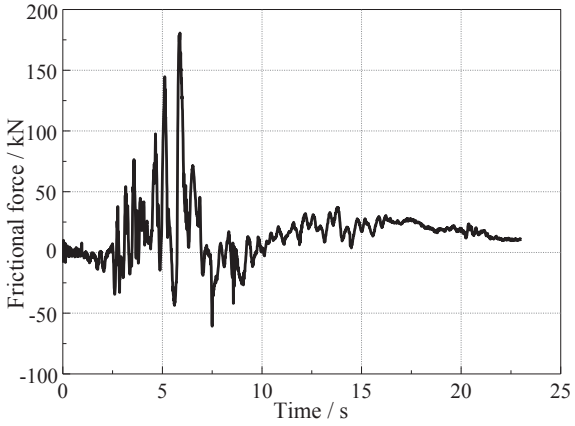

Fig. 15. Frictional force of the isolation bearing.

earthquake; this is because the horizontal ground motion exists a peak value at this time. Moreover, the frictional force increases to 180 kN shown in Fig. 15. The value is in good agreement with the loading capacity of column obtained from Table 1. There is another peak sliding displacement 0.048 m around 9.50 s. Likewise, the horizontal ground motion also exists a peak value at this time.

It is known that sliding isolation bearing devices do not change the inherent properties of structures (Berger, 2002). Therefore, the deformation with the column deformation (shown in Fig. 13) plus the sliding displacement (shown in Fig. 14) is calculated and called total deformation. The total deformation is used to illustrate the seismic responses of underground structure without retrofitted. The maximum total deformation is 0.073 m. Column deformation shown in Fig. 13 is replaced by total deformation, and is presented in Fig. 16. Seismic response of the column presents that the column is closer to its loading capacity. In other words, if the structure is not retrofitted by the bearings, the underground structure may be destroyed under the earthquake.

4.2. Seismic response of the whole structure

As discussed above, the maximum total deformation of the column retrofitted with the bearings is still smaller than that without bearings shown in Fig. 17. This is because the seismic performance of the whole structure was improved by installing sliding bearings. Horizontal deformations of the lateral walls were selected as an indicator to illustrate the seismic responses of the whole structure. Fig. 17 also presents that most of the horizontal deformations of the lateral walls without bearing occur after the failure of the column. However, for the retrofitted

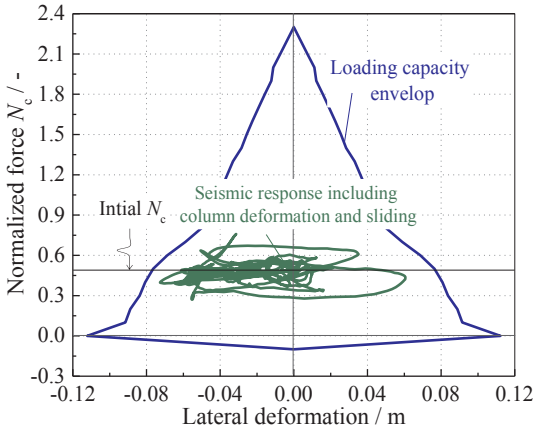

Fig. 16. Seismic response of the column deformation plus sliding displacement.

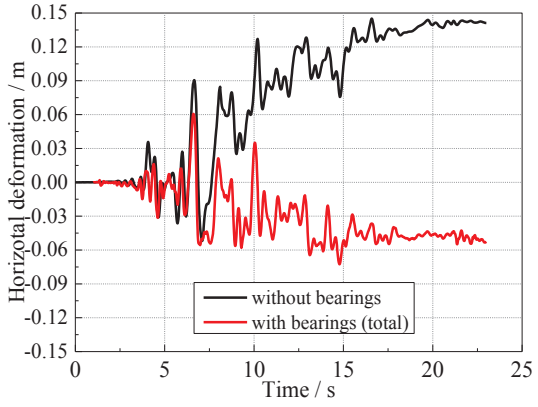

(a) Column

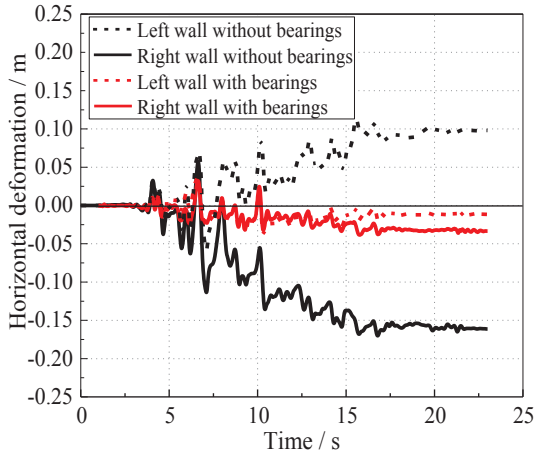

(b) Walls

Fig. 17. Horizontal deformation time histories of the column and lateral walls.

structure, the column is not destroyed, and then the horizontal deformations of the walls did not increase significantly. Comparing with the structure without retrofitted, adding the sliding bearings brings about a 58% reduction in the final deformation of the walls. The drift ratios of the column and walls at 6.5 s and 23.0 s are calculated, and the values are presented in Fig. 18. It can be found that by adding sliding bearings to underground structure, drift ratios decreased in all vertical load carrying structural components. At 6.5 s, 60% drift ratio of the column is reduced. Moreover, the residual drift ratios reductions of the column and walls are the range of 70% to 88%.

4.3. Seismic response of the structure influenced by frictional coefficient

Nonlinear seismic analyses of the Daikai Station retrofitted by the Pure-Friction-System bearings with $\mu = 0.04$, 0.06, 0.08 and 0.10 were conducted. The numerical results of the bearings with $\mu = 0.02$ are together applied to study the seismic response of the structure influenced by frictional coefficient. Fig. 19 presents the relations between the frictional coefficient and horizontal deformation of column and sliding displacement of the bearing. With the increase of frictional coefficient, the sliding displacement of the bearing decease quickly, and the maximum horizontal deformation of the column increases sharply especially when $\mu > 0.08$. However, when columns are fixed with the beams, the sliding displacement is zero and the horizontal deformation of the column is 0.14 m. Therefore, relations between friction coefficient and deformation of the column could be fitted by curves shown in Fig. 19. Using sliding bearings to retrofit underground structures is an effective way for enhancing their anti-seismic capacity. To ensure the

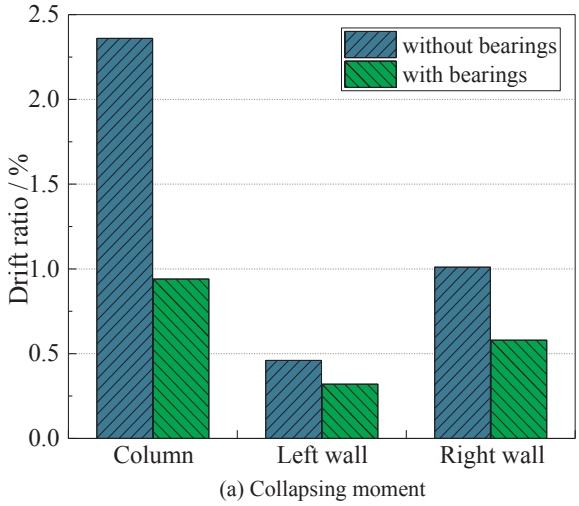

(a) Collapsing moment

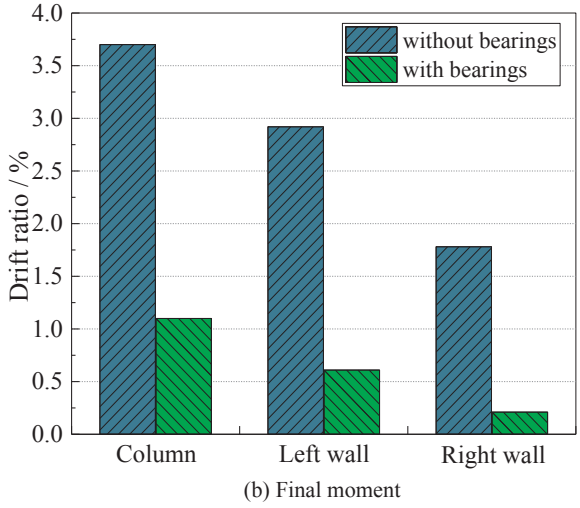

(b) Final moment

Fig. 18. Drift ratios for structural components.

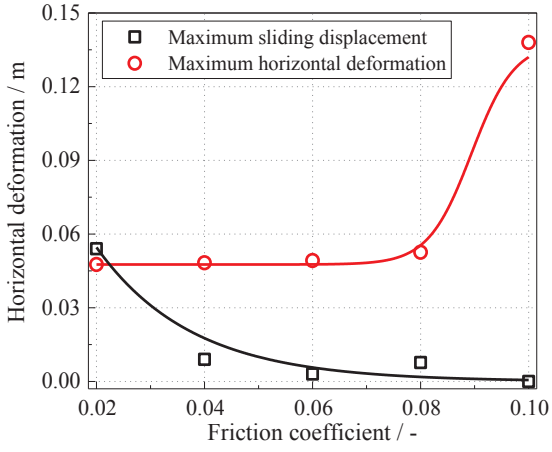

Fig. 19. Relation between friction coefficient and deformation of the column.

efficiency of the Pure-Friction-System, a reasonable range of the frictional coefficient must be determined. The deformation capacity of the column ranges from 0.05 m to 0.08 m when $0.4 < N_c < 0.7$, thus, as presented in Fig. 19, for structures like the Daikai station, the frictional coefficient of bearing should be smaller than 0.08. The frictional coefficient obtained by numerical simulation coincides with the results in Table 1.

5. Conclusion

In this study, the sliding isolation bearing was introduced to underground structures to enhance the anti-seismic capacity. Firstly, the collapse mechanism of underground structures was analyzed by taking the Daikai Station as an example. It was concluded that the collapse of underground structures originated from the poor ductility of columns at high normalized force state. Reducing the lateral deformation of columns was an effective approach to mitigating seismic damage of underground structures from earthquakes. Therefore, Pure-Friction-System bearings with low friction coefficient were installed in underground structures to assess the seismic performance of the retrofitted structures.

Numerical results showed that the sliding bearing in the retrofitted underground structures worked well during earthquakes. The sliding of the bearing decreased remarkably the lateral deformation of the column when $\mu = 0.02$. Consequently, the columns worked within their loading capacity, which makes the deformations of the lateral walls were also reduced. Therefore, sliding bearings is the effective device to improve the anti-seismic capacity of underground structures. In addition, the deformations of the whole structure and the components were all greatly influenced by the frictional coefficient, thus, to give an optimum range of the frictional coefficient is important for the design of bearings. In other words, the determination of the frictional coefficient is the key issue to keep the column stand straightly and to prevent the collapse of underground structures. Further, from this study, it can also be concluded that the technologies of seismic mitigation and isolation using in above ground structures can also be applied to underground structures for aseismic design.

Acknowledgement

This study was supported by the National Key Research and Development Program of China (Grant No. 2016YFC0701104), the National Natural Science Foundation of China (Grant Nos. 51522802, 51778026 and 51421005), the Beijing Postdoctoral Research Foundation (2017-zz-064), the Beijing Municipal Natural Science Foundation (8184067), the National Natural Science Foundation of Beijing (8161001), Program for Changjiang Scholars and Innovative Research Team in University and Beijing Advanced Innovation Center for Future Urban Design, Beijing University of Civil Engineering and Architecture.

References

An, X., Maekawa, A.A., Shawky, K., 1997. The collapse mechanism of a subway station during the Great Hanshin Earthquake. Cem. Concr. Compos. 19 (3), 241–257.
Berger, E.J., 2002. Friction modeling for dynamic system simulation. Appl. Mech. Rev. 55 (6), 535–577.
Buckle, I.G., Mayes, R.L., 1990. Seismic isolation: history, application, and performance-a world view. Earthquake Spectra 6 (2), 161–201.
Castaldo, P., Palazzo, B., Della, V.P., 2015. Seismic reliability of base-isolated structures with friction pendulum bearings. Eng. Struct. 95, 80–93.
Chen, G.X., Chen, S., Du, X.L., Lu, D.C., Qi, C.Z., 2016. Review of seismic damage, model test, available design and analysis methods of urban underground structures: Retrospect and prospect. J. Disaster Prevention Mitigation Eng. 36 (1), 1–23 (in Chinese).
Chen, Z.Y., Chen, W., Bian, G.Q., 2014. Seismic performance upgrading for underground structures by introducing shear panel dampers. Adv. Struct. Eng. 17 (9), 1343–1357.
Chen, Z.Y., Shen, H., 2014. Dynamic centrifuge tests on isolation mechanism of tunnels subjected to seismic shaking. Tunn. Undergr. Sp. Tech. 42, 67–77.
Ding, J.H., Jin, X.L., Guo, Y.Z., Li, G.G., 2006. Numerical simulation for large-scale seismic response analysis of immersed tunnel. Eng. Struct. 28 (10), 1367–1377.
Do, N.A., Dias, D., Oreste, P., Djeran-Maigre, I., 2015. 2D numerical investigation of segmental tunnel lining under seismic loading. Soil Dyn. Earthq. Eng. 72, 66–76.
Fenz, D.M., Constantinou, M.C., 2006. Behavior of the double concave friction pendulum bearing. Earthq. Eng. Struct. Dyn. 35, 1403–1424.
Hashash, Y.M.A., Hook, J.J., Schmidt, B., Yao, J.I.C., 2001. Seismic design and analysis of underground structures. Tunn. Undergr. Sp. Tech. 16, 247–293.
Hasheminejad, S.M., Miri, A.K., 2008. Seismic isolation effect of lined circular tunnels with damping treatments. Earthq. Eng. Eng. Vib. 7 (3), 305–319.
Huan, Y., Fang, Q., Chen, L., Liu, J.C., 2011. 3D nonlinear damage analysis of metro-station structures under strong seismic loading. J. Beijing Univ. Technol. 37 (6), 852–862 (in Chinese).
Huo, H.B., Bobet, A., Fernández, G., Ramírez, J., 2005. Load transfer mechanisms between underground structure and surrounding ground: evaluation of the failure of the Daikai station. J. Geotech. Geoenviron. 131 (12), 1522–1533.
Iida, H., Hiroto, T., Yoshida, N., Iwafuji, M., 1996. Damage to Daikai subway station. Soils Found (Special Issue), 283–300.
Ismail, M., Rodellar, J., Ikhouane, F., 2010. An innovative isolation device for aseismic design. Eng. Struct. 32 (4), 1168–1183.
Kawamata, Y., Nakayama, M., Towhata, I., Yasuda, S., 2016. Dynamic behaviors of underground structures in E-Defense shaking experiments. Soil Dyn. Earthq. Eng. 82, 24–39.
Kim, D.S., Konagai, K., 2001. Key parameters governing the performance of soft tunnel coating for seismic isolation. Earthquake Eng. Struct. Dyn. 30 (9), 1333–1343.
Kiryu, S., Murono, Y., Morikawa, H., 2012. Seismic response of a cut-and-cover tunnel isolated by polymer material. Earthq. Eng. Struct. Dyn. 41 (14), 2043–2057.
Konagai, K., Kim, D.S., 2001. Simple evaluation of the effect of seismic isolation by covering a tunnel with a thin flexible material. Soil Dyn. Earthq. Eng. 21 (4), 287–295.
Lee, T.H., Park, D., Nguyen, D.D., Park, J.S., 2016. Damage analysis of cut-and-cover tunnel structures under seismic loading. Bull. Earthquake Eng. 14, 413–431.
Li, G., Li, H.N., 2011. Seismic response analysis of structure with energy dissipation devices using force analogy method. Struct. Des. Tall Special Build. 20 (3), 291–313.
Li, T.B., 2012. Damage to mountain tunnels related to the Wenchuan earthquake and some suggestions for aseismic tunnel construction. B. Eng. Geol. Environ. 71 (2), 297–308.
Liao, Z.H., 2013. Theories of Wave Motion for Engineering. Published by Science Press of China.
Lu, D.C., Ma, C., Du, X.L., Jin, L., Gong, Q.M., 2017. Development of a new nonlinear unified strength theory for geomaterials based on the concept of characteristic stresses. Int. J. Geomech., ASCE 17 (2), 1–11.
Ma, C., Lu, D.C., Du, X.L., Zhou, A.N., 2017a. A new approach to developing a 3D elastoplastic constitutive model for soils. Comput. Geotech. 86 (1), 129–140.
Ma, C., Lu, D.C., Du, X.L., Qi, C.Z., 2017b. Effect of buried depth on seismic response of rectangular underground structures considering the influence of ground loss. Soil Dyn. Earthq. Eng. http://dx.doi.org/10.1016/j.soildyn.2017.12.021.
Mikami, A., Konagai, K., Sawada, T., 2001. Stiffness design of isolation rubber for center columns of tunnel. Doboku Gakkai Ronbunshu 682, 415–420 (in Japanese).
Mualla, I.H., Belev, B., 2002. Performance of steel frames with a new friction damper device under earthquake excitation. Eng. Struct. 24 (3), 365–371.
Nagarajaiah, S., Riley, M.A., Reinhorn, A., 1993. Control of sliding-isolated bridge with absolute acceleration feedback. J. Eng. Mech. 119 (11), 2317–2332.
Nam, S.H., Song, H.W., Byun, K.J., Maekawa, K., 2016. Seismic analysis of underground reinforced concrete structures considering elasto-plactic interface element with thickness. Eng. Struct. 28, 1122–1131.
Providakis, C.P., 2009. Effect of supplemental damping on LRB and FPS seismic isolators under near-fault ground motions. Soil Dyn. Earthq. Eng. 29 (1), 80–90.
Sharma, S., Judd, W.R., 1991. Underground opening damage from earthquakes. Eng. Geol. 30 (3–4), 263–276.
Shen, Y., Gao, B., Yang, X., Tao, S., 2014. Seismic damage mechanism and dynamic deformation characteristic analysis of mountain tunnel after Wenchuan earthquake. Eng. Geol. 180, 85–98.
Suzuki, T., 2000. The axisymmeteric finite element model developed as a measure to evaluate earthquake responses of seismically isolated tunnels. In: 12th World Conference on Earthquake Engineering, Auckland, New Zealand.
Wang, W.L., Wang, T.T., Su, J.J., Lin, C.H., Seng, C.R., Huang, T.H., 2000. Assessment of damage in mountain tunnels due to the Taiwan Chi-Chi earthquake. Tunn. Undergr. Sp. Tech. 16, 133–150.
Wang, Z., Gao, B., Jiang, Y., Yuan, S., 2009. Investigation and assessment on mountain tunnels and geotechnical damage after the Wenchuan earthquake. Sci. China Technol. Sci. 52 (2), 546–558.
Wang, Z.Z., Jiang, Y.J., Zhu, C.A., 2017. Seismic energy response and damage evolution of tunnel lining structures. Eur. J. Environ. Civ. Eng. 1–13.
Xin, C.L., Gao, B., Zhou, J.M., Shen, Y.S., 2014. Shaking table tests of conventional anti-seismic and damping measures on fault-crossing tunnels. Chin. J. Rock Mech. Eng. 33 (10), 2017–2025 (in Chinese).
Yashida, N., Nakamura, S., 1996. Damage to Daikai subway station during the 1995 Hyogoken-Nunbu Earthquake and its Investigation. In: 11th World Conference on Earthquake Engineering, 2151, pp. 283–300.
Yu, H., Yuan, Y., Qiao, Z., Gu, Y., Yang, Z., Li, X., 2013. Seismic analysis of a long tunnel based on multi-scale method. Eng. Struct. 49, 572–587.
Yu, H., Xiao, W., Yuan, Y., Taerwe, L., 2017. Seismic mitigation for immersion joints: Design and validation. Tunn. Undergr. Sp. Tech. 67, 39–51.